

DOI 10.24425/ae.2019.125978

# Magnetization dependent demagnetization characteristic of rare-earth permanent magnets

GREGOR BAVENDIEK, FABIAN MÜLLER,  
JAMSHID SABIROV, KAY HAMEYER

*Institute of Electrical Machines (IEM)  
RWTH Aachen University  
Schinkelstraße 4, 52056 Aachen, Germany  
e-mail: gregor.bavendiek@iem.rwth-aachen.de*

(Received: 19.09.2018, Revised: 25.10.2018)

**Abstract:** Accurate demagnetization modelling is mandatory for a reliable design of rare-earth permanent magnet applications, such as e.g. synchronous machines. The magnetization of rare-earth permanent magnets requires high magnetizing fields. For technical reasons, it is not always possible to completely and homogeneously achieve the required field strength during a pulse magnetization, due to stray fields or eddy currents. Not sufficiently magnetized magnets lose remanence as well as coercivity and the demagnetization characteristic becomes strongly nonlinear. It is state of the art to treat demagnetization curves as linear. This paper presents an approach to model the nonlinear demagnetization in dependence on the magnetization field strength. Measurements of magnetization dependent demagnetization characteristics of rare-earth permanent magnets are compared to an analytical model description. The physical meaning of the model parameters and the influence on them by incomplete magnetization are discussed for different rare-earth permanent magnet materials. Basically, the analytic function is able to map the occurring magnetization dependent demagnetization behavior. However, if the magnetization is incomplete, the model parameters have a strong nonlinear behavior and can only be partially attributed to physical effects. As a benefit the model can represent nonlinear demagnetization using a few parameters only. The original analytical model is from literature but has been adapted for the incomplete magnetization. The discussed effect is not sufficiently accurate modelled in literature. The sparse data in literature has been supplemented with additional pulsed-field magnetometer measurements.

**Key words:** demagnetization, magnetic hysteresis, magnetization processes, permanent magnets

## 1. Introduction

High energy rare-earth magnets are commonly applied to many applications ranging from electro-mechanical devices to sensors [1]. The virgin material magnetization requires the application of magnetic fields up to several kA/m. As a rule of thumb, at least a magnetizing field strength of approximately three times the coercive force is required for complete magnetization. To achieve sufficiently high magnetizing fields in the magnetizing coils the currents are in the range of several hundreds of kA, which can be generated by pulse magnetizers [2, 3].

Models for ferromagnetic magnetization processes are based on empirical, phenomenological, fundamental physics or energy-based approaches. State-of-the-art hysteresis models, such as Jiles-Atherton [4] or Play/Stop hysterons [5], have been adapted to predict the behavior of hard magnetic materials. These approaches generally work for fully (pre-) magnetized samples, while the interdependency of the virgin magnetization process and the demagnetization are still challenging. In this paper, a mathematical/empirical demagnetization model dependent on virgin magnetization, is proposed, parametrized and validated on measurements.

## 2. Permanent magnets

### 2.1. Materials

Permanent magnet materials are ferrites, AlNiCo and rare-earth magnets, namely SmCo or NdFeB. They are composed of several elements and therefore expose a complex crystalline structure. Ferrites are a ceramic composite material made of  $\text{Fe}_2\text{O}_3$  and barium, strontium or lead, with a low remanence of up to 0.4 T and a coercive field strength of  $H_C = 100$  kA/m. AlNiCo magnets are composed of aluminum, nickel and cobalt. They possess a remanence with up to 1.3 T and a coercive field strength below 100 kA/m. They are not air-stable which needs to be considered during magnetic circuit design. The technical feasible rare-earth permanent magnets possess a high energy product and are composed from either a combination of samarium with cobalt or neodymium (or other lanthanides) with iron and boron. The remanence of these rare earth permanent magnets can be up to 1.5 T for NdFeB and 1.2 T for SmCo and the coercive field strength is at NdFeB at around the 800 ka/m, as well as at 600 ka/m at SmCo.

### 2.2. Magnetization process

Permanent magnets possess no remanent magnetization after manufacturing process. They can be magnetized by imprinting very high field strengths to saturate the magnetic domains. In order to achieve this, an impulse magnetizer is the device of choice that consists of an interconnection of capacitors which are charged and then discharged over a magnetization coil via a thyristor. The stored energy in the capacitors must be sufficient to supply the permanent magnet with its magnetic energy and in addition capture the losses during transient magnetization process. In [6] and [7], this process is considered simulative, with no remanence taken into account, in contrast to [8] which also takes into account the remanent polarization of the permanent magnet

during the magnetization process, allowing a more accurate calculation and description of local demagnetization effects.

While the magnetization behavior of soft magnetic material is described in detail in literature, however, with regard to permanent magnets, their demagnetization behavior is considered as (linear) relation [9]. During and after being magnetized the permanent magnets suffer from self-demagnetization, which can be expressed in air by the form factor or in matter by the load line [10]. The demagnetization curves of rare-earth permanent magnets are a function of magnetizing field strength  $H_{\text{mag}}$  due to the so called coercivity effect during magnetization reversal [11–15]. Especially for *nucleation type* magnets minor loops are highly nonlinear [16].

The magnetization curve of a permanent magnet is outlined in Fig. 1. Starting from virgin state, the magnetization with ascending magnetic field along the curve to point A rises. If the magnetic field is now lowered, the magnetization moves towards the point B. If the knee field strength is not exceeded (above point B), the demagnetization returns comparable to the way it came if the field strength is increased again. If the field strength is further lowered, the knee field is passed, and irreversible demagnetized point B is reached. If the field is now raised again, the curve is traversed to point C. To obtain the same magnetization of point A, a higher field strength is now necessary, since the magnetization of the aligned domains must be reversed. If the magnetization of the sample is completely reversed (see point D), the complete hysteresis must be traversed to reach point E. To completely demagnetize magnets again, they must be heated above the Curie temperature, because this causes the electron spins to reorient themselves anew and randomly form. Some materials also lose their anisotropic crystal structure if heated up to Curie temperature and remain non-magnetic without a renewed heat treatment for crystal structure recovery. Electrically demagnetized permanent magnets never recover the virgin magnetization, because their domain walls have changed sustainably.

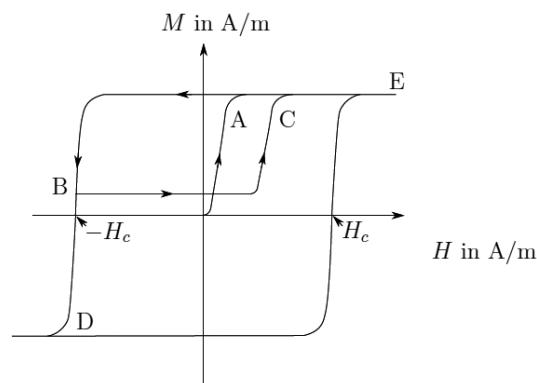


Fig. 1. Hard magnetic hysteresis  $M(H)$  based on [17]

To derive a description of permanent magnet material magnetization, it is necessary to understand the occurring magnetization processes which are distinguished in two principles. On the one hand the *nucleation* and on the other hand the *pinning type*. The phenomenon of *nucleation*

occurs in materials whose grain size is greater than a material-dependent, critical radius [17]

$$r_c = \frac{\pi\gamma}{\partial\mu_0 M^2}.$$

$\gamma$  describes a space-related energy contained in the domain wall and  $M$  is the magnetic moment. If the radius is greater than calculated in the previous equation, a resulting domain wall reduces the energy within a grain. The loss energy has flowed into the construction of the domain wall. Because of this, it is energetically favorable when a domain wall is contained in the grain. As a result, the wall can be moved within the grain with little energy. Thus, magnets that work according to this principle are easy to magnetize. The magnetization for a completely magnetized sample remains constant in a declining field until the nucleus is formed, the magnetization of which corresponds to the field direction. At this point, the magnetization of the magnet turns. Materials of this type include, among others,  $\text{SmCo}_5$  and  $\text{NdFeB}$ . *Pinning* occurs in  $\text{Sm}_2\text{Co}_{17}$ , for example. Inside the grains of this material are many small cells of the phase  $\text{Sm}_2\text{Co}_{17}$ , which are limited by  $\text{SmCo}_5$ . Due to this cell-like structure, it is more difficult to create a shift of domain walls because they are held on the internal structure and this makes movement more difficult. Fig. 2 illustrates the different magnetization behavior.

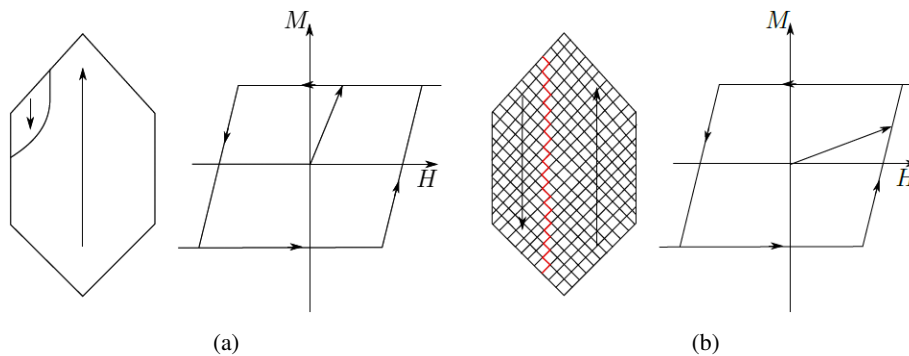


Fig. 2. Grain and magnetization curve of (a) *nucleation* and (b) *pinning* type [17]

### 2.3. Measurement of nonlinear demagnetization

Permanent magnet manufacturers usually provide the demagnetization curve in the second quadrant of magnetic polarization or flux density over magnetic field strength for different temperatures of a completely magnetized magnet. These measurements are performed with a closed magnetic circuit as defined in standard (IEC-60404-5). The closed-loop measurement is only able to impose a magnetic field lower than the saturation field of the soft magnetic yoke material. Therefore, the measuring device is not able to completely magnetize rare-earth hard magnetic material, which is why the samples are pre-magnetized by a pulse magnetizer and only demagnetized in the measuring device. The company VACUUMSCHMELZE offers demagnetization curves of their rare-earth magnets as a function of magnetizing field in their product catalogue [18] for four different materials: Vacodym code 362/140 (NdFeB), Vacomax 170HR, Vacomax 240HR and Vacomax 225HR, which are examined in this paper.

In a previous article [19], rare-earth permanent magnet samples were examined with the pulsed field magnetometer HyMpulse from Metis. Although the measuring system only follows the pre-standard (IEC-V 42331), it offers the big advantage to measure and impress high magnetic field strength up to several thousand kilo Amperes. As a drawback eddy currents need to be eliminated from measurements. In this paper the magnetization dependent demagnetization is discussed for Vacodym764AP listed in Table 1.

Table 1. Rare-earth permanent magnet samples measured with pulsed-field magnetometer

Name	Vacodym764
Pressing direction	AP
Material	NdFeB
Magnetization type	<i>nucleation</i>
Code (IEC 60404-8-1)	305/135.5
Min. remanence $B_r$ in T	1.3
Min. coercivity $H_{cJ}$ in kA/m	1275
Shape	cylinder
Size in mm	15 × 5.5
Demagnetization coefficient	0.55

#### 2.4. Modelling of nonlinear demagnetization

A suitable model which considers the nonlinear demagnetization including temperature dependence can be found in [20], which describes an equation that is closely related to the Takács' hysteresis model [21]. Since the temperature dependence is not to be considered here, but instead an additional term for the incomplete polarization is added, the assumed equation is as follows:

$$J(H) = b_0 \tanh\left(\frac{H + H_d}{h_0}\right) + b_1 \tanh\left(\frac{H + H_d}{h_1}\right) + b_{\text{shift}}. \quad (1)$$

Originally  $b_{0,1}$  and  $h_{0,1}$  are constant coefficients identified by a nonlinear curve fitting. They will be varied to trace the dependency of  $B_r$  and  $H_c$  to  $H_{\text{mag}}$ . The nonlinear dependence of  $B_r$  and  $H_c$  on  $H_{\text{mag}}$  can be approximated by a sigmoid function, as described by the following equation:

$$[B_r H_c](H_{\text{mag}}) = \frac{[B_r H_c]_{\text{sat}}}{\left(1 + \exp\left(\frac{(H_{\text{mag}}[B_r H_c]_{\text{max}} - H_{\text{mag}})}{c_F}\right)\right)}, \quad (2)$$

$$c_F = \frac{[B_r H_c]_{\text{sat}}}{(4 \cdot [B_r H_c]_{\text{max}})}.$$

It is necessary to know the saturation value and the greatest slope and corresponding  $H_{\text{mag}}$ . Fig. 3 portrays the influence of the different coefficients for the shape of (a) the double-tanh and (b) the sigmoid function.

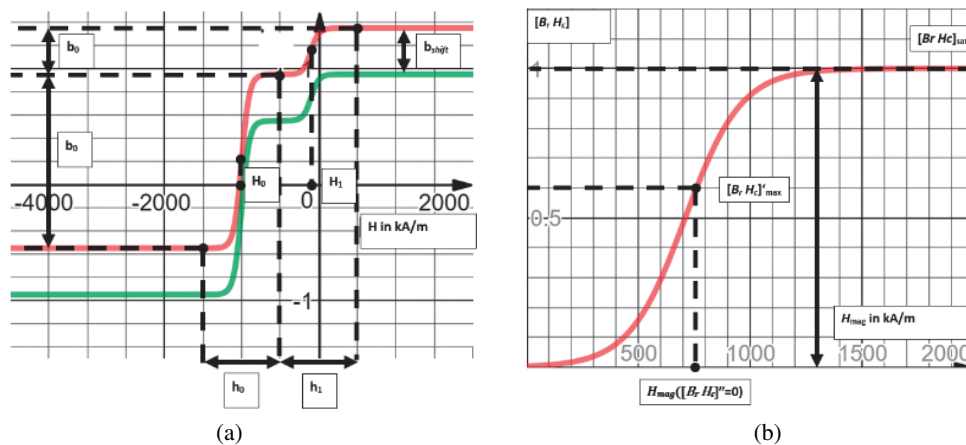
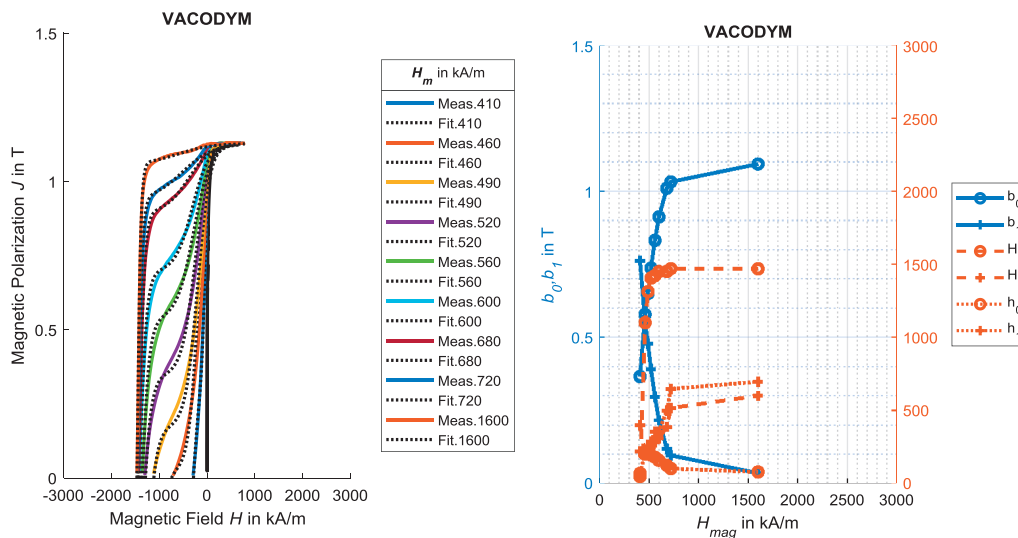


Fig. 3. Influence of coefficients for (a) the double-tanh and (b) the sigmoid function

### 3. Comparison of demagnetization measurements and modelling

Fig. 4 shows on the left side the measurements from the VACUUMSCHMELZE catalogue and of Vacodym764AP from pulsed-field magnetometer (as full lines) and their double-tanh approximation (as dashed lines), as well as on the right side the change of the fitted coefficients.

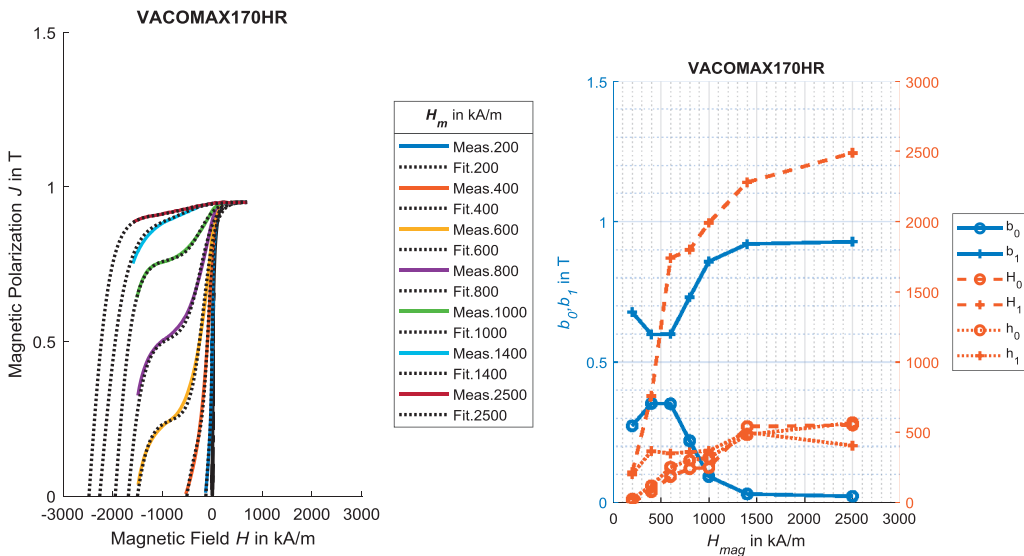
The study shows that the magnetization field strength dependent demagnetization is qualitatively well modelled by the selected analytical function. However, the analytical model is



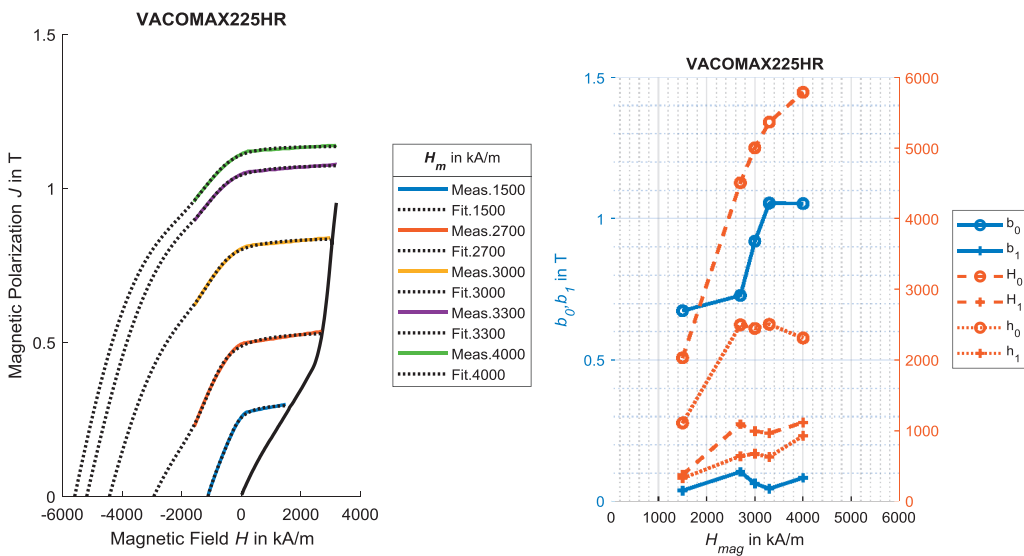
(a) Vacodym code 362/140

Fig. 4.

intended to enable a predictive or nonlinear interpolation of the different demagnetization curves. Therefore, the course of the individual coefficients of the fitted curves needs to be identified. The dispersion is very pronounced so that no general trend can be identified.

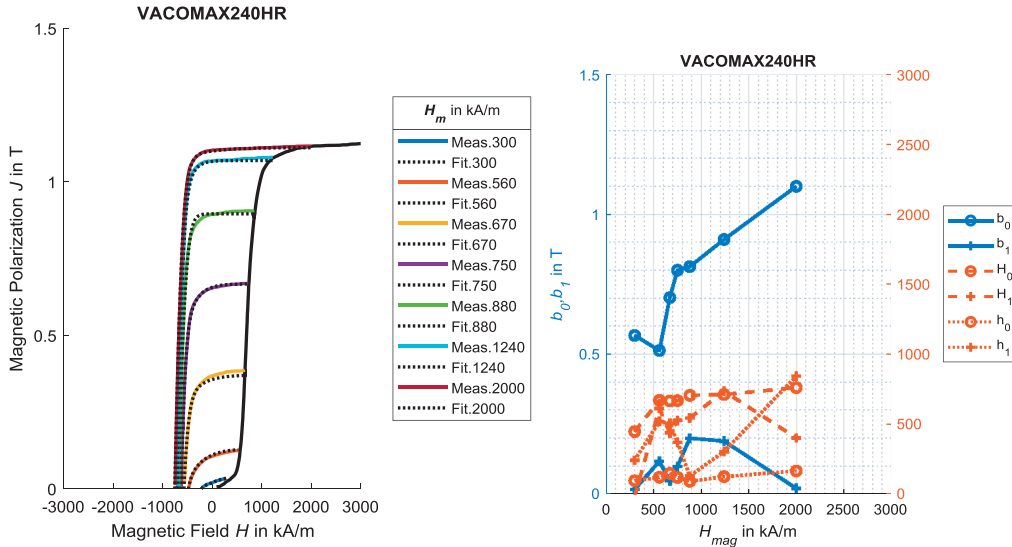


(b) Vacomax170HR

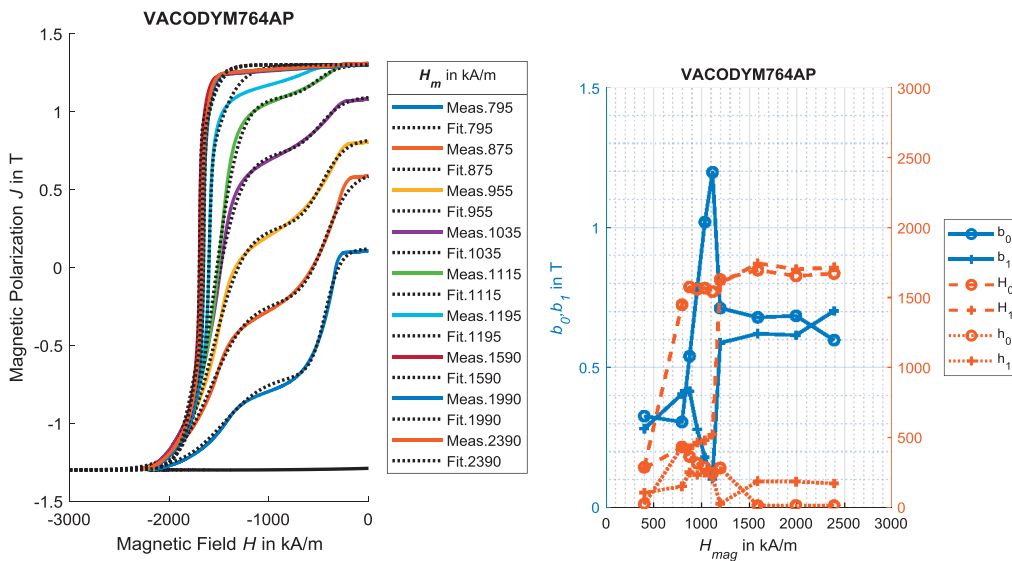


(c) Vacomax225HR

Fig. 4.



(d) Vacomax240HR



(e) Vacodym764AP

Fig. 4. Fit of demagnetization with the double-tanh function and the change of fitted coefficients

The demagnetization curves of the *pinning* material are monotonic and uniform, which allows them to be described by a common function based on a transplantation of the major demagnetization line. This can be predicted due to the fact that one of the terms of the double-tanh is negligible ( $< 0.1$  T) with these magnets. New values for the support points ( $H_c, 0$ ),

$(0, B_r), (H_{mag}, B_{mag})$  can be derived for incomplete magnetization, firstly, with the help of the sigmoid function, which describes the remanent magnetic flux density  $B_r$  in T and secondly, the coercive field strength  $H_c$  in kA/m for different magnetization field strengths  $H_{mag}$  kA/m. The extracted curves and their approximations are shown below (Fig. 5).

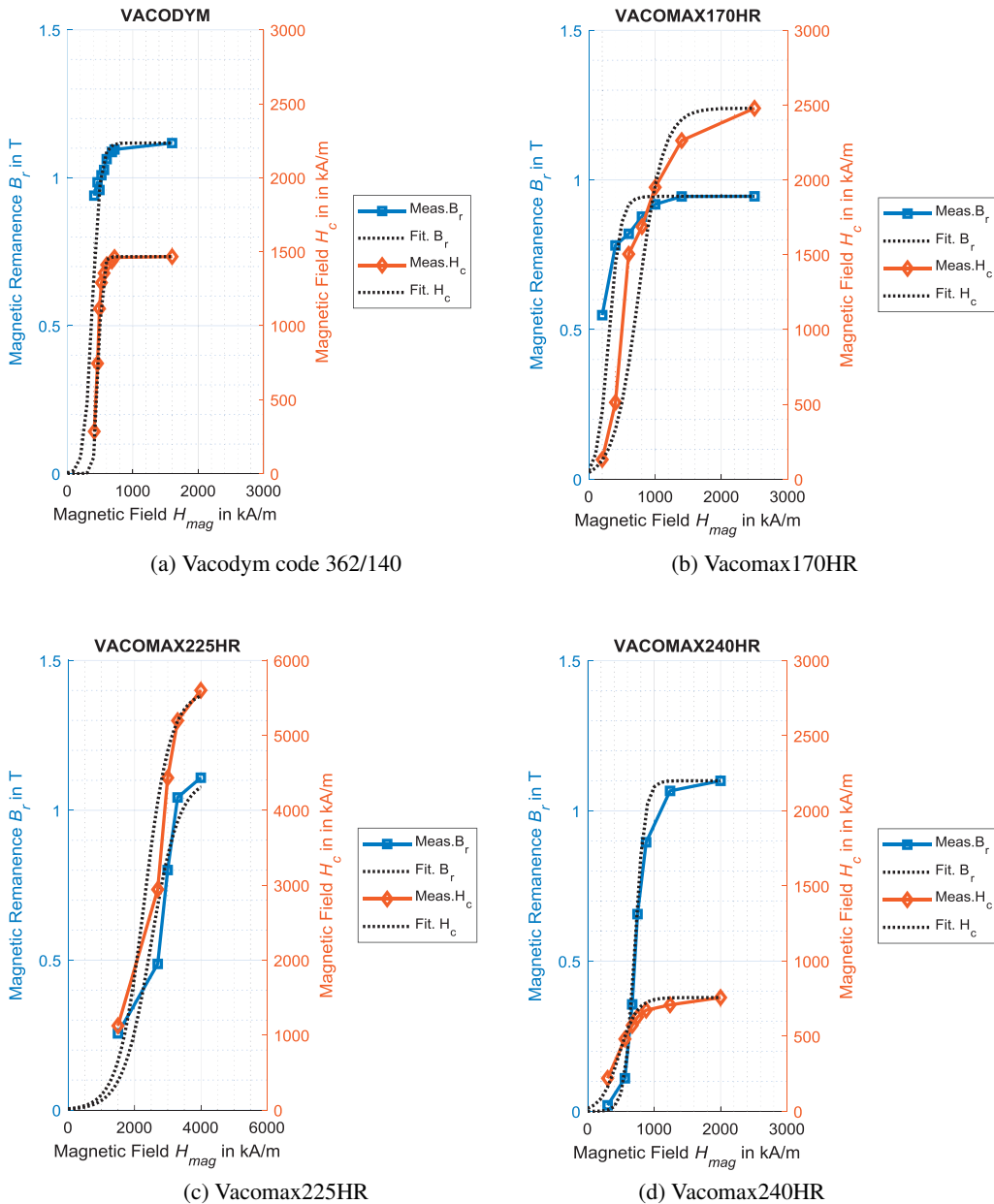
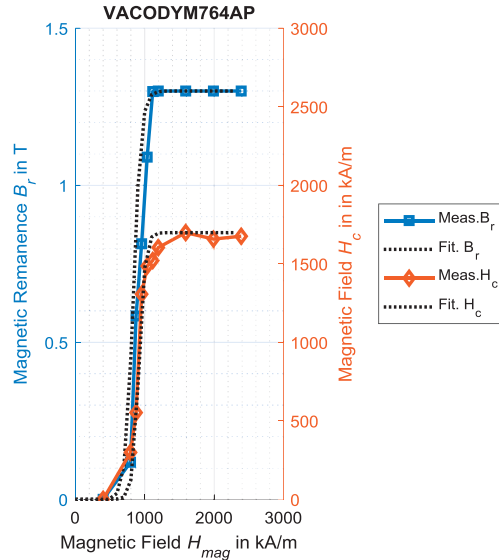


Fig. 5.



(e) Vacodym764AP

Fig. 5.  $B_r$  and  $H_c$  for different magnetization field strengths  $H_{mag}$ 

#### 4. Extension for inner loops with nonlinear de-/re-magnetization

The nonlinear demagnetization model only covers a descending magnetization behavior. To extend the model for ascending magnetization the measured demagnetization curves and corresponding extensions to full reversal are mirrored in the origin. This does not create closed-loop minor loops, but there are both demagnetizing and demagnetizing curves in all four quadrants. If one now transfers this behavior on the basis of the current magnetization field strength and transplants the magnetization behavior accordingly at each point, then one obtains a closed model for minor loops within not completely magnetized magnets.

This approach is very similar to the Takács hysteresis model [22]. The hysteresis model proposed by Takács is phenomenological motivated and possesses with the tanh as basis function a closely related mathematical equation to the demagnetization model. It has already been successfully applied to permanent magnets [19, 23]. The Takács model is based on the approximation of magnetization and related to the Langevin or Brillouin function. The hysteresis is divided into an ascending

$$f_+(x) = \tanh(x - a_0) + b_1$$

and descending

$$f_-(x) = \tanh(x - a_0) - b_1$$

branch. The coefficients can be derived by

$$f_+(a_0) = 0$$

and

$$b_1 = (\tanh(x_m + a_0) - \tanh(x_m - a_0)) \div 2,$$

with  $x_m$  as peak value of  $f_+$ . The minor loops are described by the same equation as the major loop

$$f_{\pm}(x) = \tanh(x \mp a_0) \pm c_{u,d},$$

but with a new offset value  $c_{u,d}$ . The offset can be calculated by the equation:

$$c_{u,d} = c_1 \frac{\tanh(\pm x_m \mp a_0) - \tanh(x \mp a_0)}{\tanh(\pm x_m \mp a_0) - \tanh(x_r \mp a_0)},$$

with

$$c_1 = \tanh(x_r + a_0) - \tanh(x_r - a_0) - b_1.$$

$x_r$  is the point at the major loop at which the first order return curve starts, its endpoint is at  $x_m$ . With this model, the major loop can be mapped very well, but even with first order return curves of the major loop this approach evokes problems as soon as the nonlinear magnetization behavior deviates from the simple tanh approach function [24].

The key difference from the proposed model to the Takács approach is that in the current method of resolution not only one major ascending and descending branch is transplanted, but a whole magnetization characteristic extracted from measurements is utilized. In Fig. 6, for example, the nonlinear surface interpolation of Vacomax170HR is shown in (a) and in (b) some arbitrary de- and re-magnetization lines are derived from that data for all quadrants of J(H) plane without transplantation model.

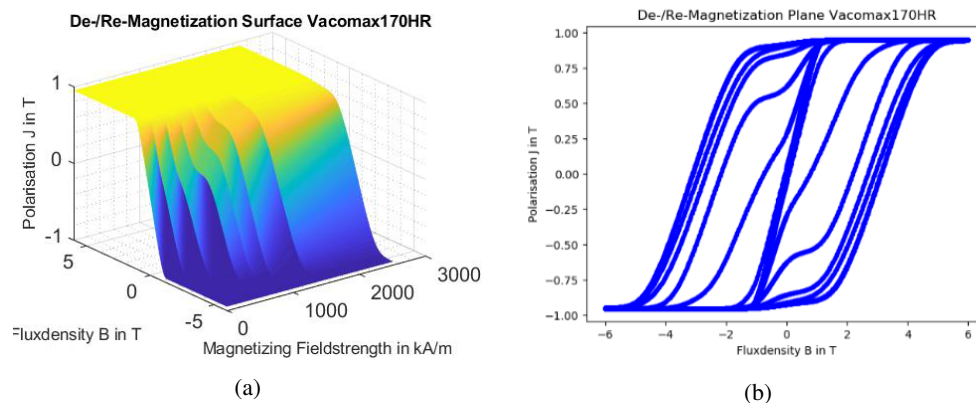


Fig. 6. Magnetization Surface of Vacomax170HR and full magnetization characteristic

The proposed model is currently used to simulate a stepwise magnetization process with nonlinear inner loops. For the first magnetization the virgin line is applied and additionally the right de-/re-magnetization characteristic is picked from the modeled magnetization surface and its transplantation. In Fig. 7 the qualitative good agreement with measured minor loops of the same material, namely Vacomax170HR, is shown. During a stepwise magnetization process the sigmoid characteristic of the remanence magnetic polarization and coercive magnetic field can clearly be seen in the soft magnetic part of magnetization at low magnetic fields, which is followed by inner loops with rising polarization levels.

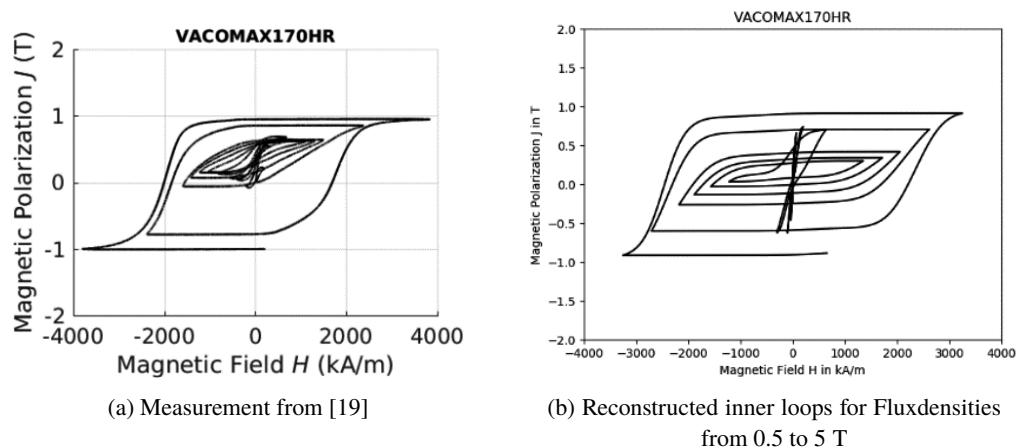


Fig. 7. Magnetization Surface of Vacomax 170HR and full magnetization characteristic

## 5. Conclusions

In this paper the measurement and modelling of nonlinear demagnetization characteristics of rare-earth permanent magnets are discussed. The dependency of demagnetization on magnetizing field strength is considered in the proposed models. The differences for the modelling of a *nucleation type* magnet and a *pinning type* magnet are portrayed. Finally a consistent model for nonlinear de-/re-magnetization of virgin permanent magnets is derived, which qualitatively models minor loops during stepwise magnetization processes.

## References

- [1] Furlani E.P., *Permanent magnet and electromechanical devices: Materials, analysis, and applications*, San Diego, California, Acad. Press (2001).
- [2] Dinca C. et al., *Characterization of a 7KJ magnetizing pulsed circuit for online quality control of permanent magnets*, in *2015 IEEE Pulsed Power Conference (PPC)*, Austin, TX, USA, pp. 1–8 (2015).
- [3] Dinca C., *Motor design for maximum material exploitation and magnetization procedure with in-line quality check for mass production*, Diss, Universitätsverlag der TU Berlin (2017).
- [4] Zhang D., Kim H.-J., Li W., Koh C.-S., *Analysis of Magnetizing Process of a New Anisotropic Bonded NdFeB Permanent Magnet Using FEM Combined With Jiles-Atherton Hysteresis Model*, *IEEE Trans. Magn.*, vol. 49, no. 5, pp. 2221–2224 (2013).
- [5] Bergqvist A., Lin D., Zhou P., *Temperature-Dependent Vector Hysteresis Model for Permanent Magnets*, *IEEE Trans. Magn.*, vol. 50, no. 2, pp. 345–348 (2014).
- [6] Kawase Y., Yamaguchi T., Mimura N., Igata M., Ida K., *Analysis of magnetizing process using discharge current of capacitor by 3-D finite-element method*, *IEEE Trans. Magn.*, vol. 38, no. 2, pp. 1145–1148 (2002).
- [7] Przybylski M., Kapelski D., Ślusarek B., Wiak S., *Impulse Magnetization of Nd-Fe-B Sintered Magnets for Sensors*, *Sensors*, vol. 16, no. 4, p. 569 (2016).

- [8] Bavendiek G., Hameyer K., Filippini M., Alotto P., *Analysis of impulse-magnetization in rare-earth permanent magnets*, JAE, vol. 57, no. 4, pp. 23–31 (2018).
- [9] Bastos J.P.A., *Magnetic materials and 3D finite element modeling*, Boca Raton, FL: CRC Press (2014).
- [10] Bozorth R.M., *Ferromagnetism*, Piscataway, New Jersey, Press John Wiley& Sons Inc., IEEE Xplore (1993).
- [11] Durst K.-D., Kronmüller H., *The coercive field of sintered and melt-spun NdFeB magnets*, Journal of Magnetism and Magnetic Materials, vol. 68, no. 1, pp. 63–75 (1987).
- [12] Richter H.J., Hempel K.A., Verhoef R., *Magnetization reversal in microscopic NdFeB single crystals*, Journal of Magnetism and Magnetic Materials, vol. 79, no. 1, pp. 113–118 (1989).
- [13] Givord D., Rossignol M.F., Taylor D.W., *Coercivity mechanisms in hard magnetic materials*, J. Phys. IV France, vol. 02, no. C3, C3-95–C3-104 (1992).
- [14] Plusa D., *Mechanism of magnetization reversal in NdFeB permanent magnets*, IEEE Trans. Magn., vol. 30, no. 2, pp. 872–874 (1994).
- [15] Kronmüller H., Parkin S.S.P., Eds., *Handbook of magnetism and advanced magnetic materials*, Chichester, John Wiley& Sons Inc. (2007).
- [16] Gabay A.M., Lileev A.S., Melnikov S.A., Menushenkov V.P., *Magnetostatic interaction in nucleation-type magnets*, Journal of Magnetism and Magnetic Materials, vol. 97, no. 1–3, pp. 256–262 (1991).
- [17] Campbell P., *Permanent magnet materials and their application*, 1st ed. Cambridge, Cambridge Univ. Press (1996).
- [18] Vacuumschmelze, *Vacodym-Vacomax*, <https://www.vacuumschmelze.com>, accessed Jun 2018.
- [19] Glehn G., Steentjes S., Hameyer K., *Pulsed-Field Magnetometer Measurements and Pragmatic Hysteresis Modeling of Rare-Earth Permanent Magnets*, IEEE Trans. Magn., vol. 54, no. 3, pp. 1–4 (2018).
- [20] Zhou P., Lin D., Xiao Y., Lambert N., Rahman M.A., *Temperature-Dependent Demagnetization Model of Permanent Magnets for Finite Element Analysis*, IEEE Trans. Magn., vol. 48, no. 2, pp. 1031–1034 (2012).
- [21] Takács J., *A phenomenological mathematical model of hysteresis*, COMPEL, vol. 20, no. 4, pp. 1002–1015 (2001).
- [22] Takács J., *Mathematics of hysteretic phenomena: The  $T(x)$  model for the description of hysteresis*, Weinheim, Wiley-VCH (2003).
- [23] Dośpiał M. et al., *Modeling the Hysteresis Loop in Hard Magnetic Materials Using  $T(x)$  Model*, Acta Phys. Pol. A, vol. 126, no. 1, pp. 170–171 (2014).
- [24] Bavendiek G., Steentjes S., Sabirov J., Hameyer K., *Magnetization models for hard magnetic material*, 8th International Conference on Magnetism and Metallurgy, Dresden, Germany, 12th to 14th 2018: proceedings, Freiberg, Universitätsverlag (2018).